This is a preprint, the final version is subject to change, of the American Mineralogist (MSA)
Cite as Authors (Year) Title. American Mineralogist, in press.
(DOI will not work until issue is live.) DOI: http://dx.doi.org/10.2138/am-2015-5024

Nuragheite, $Th(MoO_4)_2 \cdot H_2O$, the second natural thorium molybdate and its relationships to ichnusaite and synthetic $Th(MoO_4)_2$

PAOLO ORLANDI[1,2], CRISTIAN BIAGIONI[1,*], LUCA BINDI[3], STEFANO MERLINO[1]

[1] *Dipartimento di Scienze della Terra, Università di Pisa, Via S. Maria 53, I-56126 Pisa, Italy*
[2] *Istituto di Geoscienze e Georisorse, CNR, Via Moruzzi 1, I-56124 Pisa, Italy*
[3] *Dipartimento di Scienze della Terra, Università degli Studi di Firenze, Via G. La Pira, 4, I-50121 Firenze, Italy*

**e-mail address*: biagioni@dst.unipi.it

ABSTRACT

The new mineral species nuragheite, $Th(MoO_4)_2 \cdot H_2O$, has been discovered in the Mo-Bi mineralization of Su Seinargiu, Sarroch, Cagliari, Sardinia, Italy. It occurs as colorless thin {100} tabular crystals, up to 200 μm in length, associated with muscovite, xenotime-(Y), and ichnusaite, $Th(MoO_4)_2 \cdot 3H_2O$. Luster is pearly to adamantine; nuragheite is brittle, with a perfect (100) cleavage. Owing to the very small amount of available material and its intimate association with ichnusaite, density and optical properties were not measured. Electron microprobe analysis gave (wt% - mean of 6 spot analyses): MoO_3 49.38, ThO_2 45.39, H_2O_{calc} 3.09, total 97.86. On the basis of 8 O atoms per formula unit and assuming one H_2O group, in agreement with the crystal structure data, the chemical formula of nuragheite is $Th_{1.00}Mo_{2.00}O_8 \cdot H_2O$. Main diffraction lines, corresponding to multiple *hkl* indices, are [*d*(Å), relative visual intensity]: 5.28 (m), 5.20 (m), 5.04 (m), 4.756 (m), 3.688 (m), 3.546 (vs), 3.177 (s), 3.024 (m). The crystal structure study gives a monoclinic unit cell, space group $P2_1/c$, with a = 7.358(2), b = 10.544(3), c = 9.489(2) Å, β = 91.88(2)°, V = 735.8(2) Å^3, Z = 4. The crystal structure has been solved and refined to a final R_1 = 0.078 on the basis of 1342 "observed" reflections [$F_o > 4\sigma(F_o)$]. It consists of (100) layers formed by nine-fold coordinated Th-centered polyhedra and Mo-centered tetrahedra. Its crystal structure is discussed in relation to that of ichnusaite and that of synthetic orthorhombic $Th(MoO_4)_2$. The relationship between the progressive loss of water in the interlayer and the layer topology passing from ichnusaite through nuragheite to synthetic $(ThMoO_4)_2$ is examined. Nuragheite, the second thorium molybdate reported so far in nature, adds new data to the understanding of the crystal chemistry of actinide molybdates potentially forming during the alteration of spent nuclear fuel and influencing the release of radionuclides under repository conditions.

Keywords: nuragheite, new mineral species, molybdate, thorium, crystal structure, OD structure, Su Seinargiu, Sardinia, Italy.

Introduction

The element thorium (Z = 90) was first discovered by the Swedish chemist J.J. Berzelius (1779–1848), who isolated it from a sample of the silicate mineral thorite, $ThSiO_4$, found in the Langesundfjord, Norway. Since then, only few minerals in which thorium is an essential component have been described owing to its geochemical behavior (e.g., Hazen et al. 2009). On the contrary, thorium occurs in solid solution in variable and usually small amounts in many rare-earth elements, zirconium, and uranium minerals, e.g. 'monazite', 'xenotime', zircon, and uraninite (Frondel 1958). Among the twenty-two known Th minerals, molybdates have been described only recently from the Mo-Bi mineralization of Su Seinargiu, Sarroch, Cagliari, Sardinia, Italy. The preliminary screening with a scanning electron microscope of a set of specimens provided by the mineral collector Giuseppe Tanca allowed the identification of some crystals having Th and Mo as the only elements with $Z > 9$. X-ray powder diffraction patterns indicated the existence of two different Th–Mo phases, usually occurring intimately intergrown. After the examination of several crystals, two pure grains were identified allowing the intensity data collections and the solution of their crystal structures. The two Th–Mo phases represent the first natural examples of such compounds; the very first one, ichnusaite, $Th(MoO_4)_2 \cdot 3H_2O$, has been described by Orlandi et al. (2014).

In this paper we describe the second natural thorium molybdate, which was named nuragheite. The name is related to "*nuraghe*", the main type of ancient megalithic building found in Sardinia, Italy. This kind of edifice is the symbol of Sardinia and its peculiar culture, the Nuragic civilization. The mineral and its name have been approved by the IMA-CNMNC, under the number 2013-088. The holotype specimen of nuragheite is deposited in the mineralogical collection of the Museo di Storia Naturale, Università di Pisa, Via Roma 79, Calci, Pisa, Italy, under catalog number 19680.

Occurrence and mineral description

Nuragheite was identified on specimens from the Su Seinargiu prospect, Sarroch, Cagliari, Sardinia. The mineralization is composed by three vein systems, hosted in Varisic leucogranites, and is dated at 288.7 ± 0.5 My on the basis of the Re–Os age of molybdenite (Boni et al. 2003). Recently, Orlandi et al. (2013b) described more than 50 different mineral species from this locality, among which five mineral species having Su Seinargiu as type locality: sardignaite (Orlandi et al. 2010), gelosaite (Orlandi et al. 2011), tancaite-(Ce) (Bonaccorsi and Orlandi 2010), mambertiite (Orlandi et al. 2013a), and ichnusaite (Orlandi et al. 2014).

Nuragheite occurs as aggregates of colorless thin {100} tabular crystals, up to 200 μm in length (Fig. 1), with a pearly to adamantine luster. Streak is white. Nuragheite is transparent, brittle, and shows a perfect cleavage parallel to (100). Owing to the intimate intergrowth with ichnusaite and the small amount of homogeneous available material (only one very small crystal; sample 5216), hardness, density, as well as the optical properties were not measured. The calculated density, based on the empirical formula, is 5.147 $g \cdot cm^{-3}$. The mean refractive index of nuragheite, obtained from the Gladstone-Dale relationship (Mandarino 1979, 1981), using ideal formula and calculated density, is 2.07.

Nuragheite occurs in vugs of quartz veins, closely intergrown with ichnusaite. In the veins, the mineral is associated with muscovite and partially corroded crystals of xenotime-(Y). Its crystallization is probably related to the hydrothermal alteration of the Mo-Bi ore.

Chemical composition

As reported above, only one very small crystal of nuragheite (0.20 × 0.10 × 0.05 mm^3), not intergrown with ichnusaite, was available and it was used for electron-microprobe analysis. Preliminary EDS chemical analysis showed Th and Mo as the only elements with $Z > 9$. Quantitative chemical analysis was performed using a CAMECA SX50 electron microprobe operating in WDS mode. The operating conditions were: accelerating voltage 20 kV, beam current 5 nA, and beam size 1 μm; standards (element, emission line) are: metallic Mo (Mo *Lα*) and ThO_2 (Th *Mα*). Electron microprobe data are given in Table 1. On the basis of 8 oxygen atoms per formula unit (*apfu*) and assuming the presence of one H_2O group (as shown by the structural study, see below), the chemical formula of nuragheite can be written as $Th_{1.00}Mo_{2.00}O_8 \cdot H_2O$. The ideal formula corresponds to (in wt%) ThO_2 46.33, MoO_3 50.51, H_2O 3.16, sum 100.00.

X-ray crystallography and structure refinement

Single-crystal X-ray diffraction data were collected using an Oxford Diffraction Xcalibur PX Ultra diffractometer equipped with a Sapphire 3 CCD area detector. Graphite-monochromatized Mo*K*α radiation was used. Intensity integration and standard Lorentz-polarization correction were performed with the *CrysAlis* RED software package (Oxford Diffraction 2006). The program ABSPACK in *CrysAlis* RED (Oxford Diffraction 2006) was used for the absorption correction. The analysis of the systematic absences indicated the space group $P2_1/c$. The refined unit-cell parameters are $a = 7.358(2)$, $b = 10.544(3)$, $c = 9.489(2)$ Å, $\beta = 91.88(2)°$, $V = 735.8(2)$ $Å^3$, $Z = 4$. The crystal structure was solved through direct

methods using Shelxs-97 (Sheldrick 2008) and refined through Shelxl-97 (Sheldrick 2008). Scattering curves for neutral atoms were taken from the *International Tables for X-ray Crystallography* (Wilson 1992). Crystal data and details of the intensity data collection and refinement are reported in Table 2.

The positions of Th and Mo atoms were initially found, leading to $R_1 = 0.17$; the examination of the difference-Fourier map indicated some maxima around Th and Mo occurring at unrealistic distances with neighbouring atoms. The introduction of a {100} twinning (twin obliquity 1.88°) decreased the R_1 to 0.13 with a twin ratio of 75(1):25(1). Successive difference-Fourier maps allowed the correct location of all the remaining oxygen atoms. After several cycles of isotropic refinements, an anisotropic model for all the atoms but O8 was refined, achieving a final $R_1 = 0.078$ for 1342 "observed" reflections [$F_o > 4\sigma(F_o)$] and 0.079 for all 1637 independent reflections. The large electron density residuals are probably due to the low diffraction quality of the crystal(s) investigated, i.e. broad diffraction peaks and twinning, possibly connected with the order-disorder (OD) character of the compound, as discussed below. To lower the residuals, we tried to refine the crystal structure with Jana2006 (Petříček et al. 2006), which allows the use of three twinning matrices and higher-order tensors of the anisotropic displacement parameters to model the disorder (i.e., the "non-harmonic approach"; for a detailed explanation see Bindi and Evain 2007). The anharmonic atomic vibration, indeed, has been shown to give an equivalent description, but with fewer parameters, than the split-atom model in the case of disorder with highly overlapping electron densities (Kuhs 1992). This alternative approach, in particular the Gram-Charlier formalism which is recommended by the IUCr Commission on Crystallographic Nomenclature (Trueblood et al. 1996), provides an easier convergence of the refinement, due to much lower correlations between the refined parameters. However, the refinement of the nuragheite structure using this method gave rise to negative regions in the probability density function (*pdf*) maps, which clearly indicated the inadequacy of the results. It was then understood that for the nuragheite structure it was better to use only the Gaussian approximation, even though the resulting *R* factors may be higher. Atomic coordinates and displacement parameters are given in Table 3 while Table 4 reports selected bond distances.

The X-ray powder diffraction pattern of nuragheite was obtained using a 114.6 mm diameter Gandolfi camera, with Ni-filtered Cu*K*α radiation. The observed X-ray powder pattern is compared with the calculated one (obtained using the software Powder Cell; Kraus and Nolze 1996) in Table 5. Unit-cell parameters, refined on the basis of 22 unequivocally indexed reflections using UnitCell (Holland and Redfern 1997), are a = 7.386(2), b =

10.586(3), c = 9.566(2) Å, β = 92.63(2)°, V = 747.2(2) Å^3. The unit-cell parameters obtained through powder data are larger than those obtained through the single-crystal data, probably as a consequence of the low diffraction quality of the available crystal showing very broad diffraction peaks.

Crystal structure description

The crystal structure of nuragheite (Fig. 2) shows three independent cation sites, namely Th, Mo1, and Mo2, and nine independent ligand sites. The cation-centered polyhedra form (100) sheets of polymerized $ThO_8(H_2O)$ and MoO_4 polyhedra. Successive sheets are bonded through the sharing of the oxygen atoms hosted at the O2 site between the Mo2 tetrahedra and Th polyhedra. In addition, the presence of some short O···O distances not representing polyhedral edges suggests the occurrence of hydrogen bonds (see below).

Thorium atoms are bonded to eight oxygen atoms and one H_2O groups in a tricapped trigonal prismatic coordination. Average <Th–O> bond distance in nuragheite is 2.44 Å, consistent with ideal Th–O distance of 2.44 Å, assuming the ionic radii given by Shannon (1976). This bond distance is slightly shorter than those observed in minerals with nine-fold coordinated thorium, *i.e.* cheralite, $CaTh(PO_4)_2$ (Finney and Rao 1967), huttonite, $ThSiO_4$ (Taylor and Ewing 1978), and ichnusaite, $Th(MoO_4)_2 \cdot 3H_2O$ (Orlandi et al. 2014); the average <Th–O> bond distances in such compounds are 2.52, 2.51, and 2.46 Å, respectively. This results in an oversaturation of Th cations in the bond valence calculation (Table 6). Every Th-centered polyhedron is bonded to eight Mo-centered tetrahedra through corner-sharing. The free-vertex is occupied by an H_2O group (Ow7 site). Mo1 tetrahedron, as well as Mo2 tetrahedron, share all their vertices with Th-centered polyhedra. Average <Mo–O> bond distances are 1.76 and 1.78 Å for Mo1 and Mo2 sites, respectively.

As stated above, the examination of O···O distances shorter than 3 Å and not representing polyhedral edges suggest the possible existence of hydrogen bonds. In particular, two O···O distances, i.e. O4···Ow7 [2.68(3) Å] and O3···Ow7 [2.82(2) Å], may be interpreted as hydrogen bonds (Fig. 3). In both bonds, water group acts as donor; the O4···Ow7···O3 is 80.5(6)°. This value is smaller than the usual O···Ow···O angle (i.e., 107.6° – Chiari and Ferraris 1982) but it is within the range of angular values between acceptors in hydrogen bonds reported by Chiari and Ferraris (1982). Using the relationship given by Ferraris and Ivaldi (1988), O4 and O3 receive 0.24 and 0.18 valence units, respectively. The corrected bond valence sums for these sites are reported in Table 6. The valence excess at the O4 and

O6 sites, as well as the deficit at the O9 site, could be due to the relatively low quality of the diffraction data set.

Relationship between nuragheite and ichnusaite

Table 7 reports the unit-cell parameters of the known thorium molybdates. Ichnusaite and nuragheite have similar *b* and *c* parameters, related to similar configurations of the electroneutral (100) sheets of Th and Mo polyhedra. Figure 4 compares the structure of nuragheite and ichnusaite. The *a* parameter of nuragheite is shorter than that of ichnusaite and this shortening may be caused by the lower hydration state. The transition from ichnusaite to the less hydrated nuragheite can be achieved through the removal of the interlayer water groups and one of the water groups coordinating Th atoms. The latter positions is shared between one Th polyhedron and a Mo2 tetrahedron belonging to successive (100) layers in nuragheite and is occupied by oxygen atoms (O2 site). Consequently, nuragheite and ichnusaite can display the same dehydration relationships observed in other actinide compounds, e.g. in uranyl phosphates (Suzuki et al. 2005). Unfortunately, owing to the very low amount of available material, it has not been possible to verify this hypothesis yet.

The similarity between the *b* and *c* parameters of nuragheite and ichnusaite and the similar configuration of the electroneutral (100) sheets of Th and Mo polyhedra suggests the possibility of epitaxial intergrowths between these two compounds. Indeed, grains containing both nuragheite and ichnusaite were found, with a nuragheite:ichnusaite ratio of 82(1):18(1) (estimated by means of single-crystal diffraction experiments). Other phases characterized by layered structures and differing for their hydration states are known to occur closely intergrown, probably with epitaxial relationships, e.g. the copper-zinc sulfates schulenbergite and minohlite (Orlandi 2013).

Nuragheite fits the 07.GB group of Strunz and Nickel classification, *i.e.* molybdates with additional anions and/or H_2O (Strunz and Nickel 2001). It is the second known natural thorium molybdate, after ichnusaite (Orlandi et al. 2014). Among synthetic compounds, two polymorphic phases of anhydrous $Th(MoO_4)_2$ are known (Cremers et al. 1983; Larson et al. 1989), having orthorhombic and trigonal symmetry, respectively.

As hypothesized for ichnusaite (Orlandi et al. 2014), nuragheite is likely the product of the alteration of the primary Mo-Bi ore at Su Seinargiu, possibly under basic pH conditions in agreement with Birch et al. (1998), who stated that phases with tetrahedral $(MoO_4)^{2-}$ oxoanions could form at pH 7–8, under more basic conditions than do species with octahedrally coordinated Mo.

Nuragheite and synthetic orthorhombic $Th(MoO_4)_2$: an OD approach

The crystal structure of the synthetic orthorhombic $Th(MoO_4)_2$ compound has been determined by Cremers et al. (1983) in the space group *Pbca*, with a = 10.318, b = 9.737, c = 14.475 Å. The structure is shown in Fig. 5a. It may be conveniently described on the basis of the OD theory (Dornberger-Schiff 1964, 1966; Ferraris et al. 2004) as formed by two kinds of **a**,**b** layers which alternate along the **c** direction. In Fig. 5a, the subsequent layers are indicated as L_1, L_2, L_3… The odd layers, built up by the atoms O1 and O8 [the atoms are labeled as in the paper by Cremers et al. (1983)], have layer symmetry $P2_1/b2_1/m2/a$, whereas the even layers, built up by all the remaining atoms, have symmetry $P2_1/b$ 1 1. As the symmetry of the L_{2n+1} layers is higher than that of the L_{2n} layers, polytypic relationships are possible, as it will be described in the following.

In fact, there are two possible ways to relate L_{2n} and L_{2n+2} layers lying on opposite parts of L_{2n+1} layers. The first one – which is realized in the structure shown in Fig. 5a – is through the action of the symmetry operators [- 2_1 -] (a symbol indicating 2_1 axis parallel to **b**) and [- - a] (glide a normal to **c**) in L_{2n+1} layer. The second one is obtained through the action of the symmetry operators [2_1 - -] and inversion center in L_{2n+1} layer. For both resulting arrangements, pairs of adjacent layers are geometrically equivalent.

An infinite number of disorder or ordered (polytypic) sequences is possible, as a consequence of the various possible sequences of the two pairs of symmetry elements ([- 2_1 -] and [- - a] on one side, and [2_1 - -] and inversion center on the other one) operating in the L_{2n+1} layers. All these structural sequences belong to one family of OD structures consisting of two types of layers. The symmetry relationships common to all the structures in the family are described by the symbol

$$P\ 2_1/b\ 1\ 1 \qquad\qquad P\ 2_1/b\ 2_1/m\ 2/a$$
$$[0,0]$$

The first line presents the symbol of the layer groups of the constituting layers, the second line indicates the positional relationships of the adjacent layers, giving the x, y coordinates of the origin of the second layer with respect to the x, y coordinates of the origin of the first layer (Grell and Dornberger-Schiff 1982).

Among the various possible polytypes of the family, few polytypes exist which are called MDO (Maximum Degree of Order) structures: they are those polytypes which contain the smallest possible number of different kinds of layer triples. In the present case, assuming an arbitrary position of the L_{2n} layer, the positions of the preceding and subsequent layers L_{2n-}

$_1$ and L_{2n+1} are uniquely determined. Consequently, only one kind of (L_{2n-1}, L_{2n}, L_{2n+1}) triples exists. On the contrary, there are two kinds of (L_{2n}, L_{2n+1}, L_{2n+2}) triples corresponding to the two pairs of symmetry elements operating in the L_{2n+1} layer. Therefore, the smallest number of different triples necessary to build a periodic polytype is two, and only two MDO polytypes are possible in this family.

The first MDO structure (MDO_1) is obtained when the symmetry elements [- 2_1 -] and [- - *a*] are constantly operating in L_{2n+1}. In it, the asymmetric unit at *x*, *y*, *z* (I) is converted, through the action of the inversion center in L_{2n}, into the unit at -*x*, -*y*, -*z* (II); this last unit is converted by the [- 2_1 -] operator, located at $x = 0$, $z = 1/4$ in L_{2n+1}, into the asymmetric unit *x*, ½-*y*, ½+*z* (III). The units I and III are related through a glide *c* normal to **b**, located at $y = ¼$. The presence of this glide [- *c* -], of the glide [*b* - -], common operator of both layers, and of the glide [- - *a*], which is constantly operating in L_{2n+1} in this MDO structure, gives rise to the space group *P* $2_1/b$ $2_1/c$ $2_1/a$, just corresponding to the space group of the structure of $Th(MoO_4)_2$.

The other MDO structure (MDO_2) is obtained when the symmetry elements [2_1 - -] and inversion center are constantly operating in the L_{2n+1} layers. It presents space group symmetry *P* $2_1/b$ 1 1, as [$2_1/b$ - -] are common symmetry elements of both layers, with $a = 10.318$, $b = 9.737$, $c = 7.24$ Å, $\alpha = 90°$. The structure of the MDO_2 polytype is shown in Fig. 5b and closely corresponds to the structure of nuragheite, apart from the presence, in the natural compound, of an additional water group and the different reference system. Through a cyclic transformation of axes, the space group of the MDO_2 polytype becomes *P* 1 $2_1/c$ 1, with $a = 7.24$, $b = 10.318$, $c = 9.733$ Å, $\beta = 90°$, stressing the similarity of the crystal structures of the MDO_2 polytype of anhydrous $Th(MoO_4)_2$ compound and of nuragheite.

Obviously, similar OD features are displayed by nuragheite, which may present two distinct MDO polytypes, orthorhombic and monoclinic. This last polytype is realized by the structure under study. The OD character of nuragheite points to the possible presence of small orthorhombic domains, as well as of disordered sequences of the constituting layers, which may explain the low quality of the diffraction patterns of the crystals under study.

The two OD families of synthetic $Th(MoO_4)_2$ and natural $Th(MoO_4)_2 \cdot H_2O$ compounds are distinguished by the presence of the water molecule in the natural compound.

Implications

The accurate study of the mineralogy of the small Mo-Bi mineralization at Su Seinargiu, Sardinia, Italy, provided the systematic mineralogy with several new minerals,

mainly represented by molybdates. In particular, thorium molybdates are very intriguing species, owing to their first finding as natural phases and their potential environmental significance. Actinide molybdates have been indeed reported during the alteration of spent nuclear fuel (e.g., Buck et al. 1997) and, consequently, the knowledge of their crystal chemistry may add useful data to the understanding of the release of radionuclides under repository conditions. In particular, the finding of natural thorium molybdates highlighted the interesting structural relationships between ichnusaite (Orlandi et al. 2014), nuragheite, and the orthorhombic synthetic $Th(MoO_4)_2$ compound (Cremers et al. 1983), related to their hydration states. These phases are indeed characterized by a progressively lower hydration state, affecting their unit-cell parameters and, possibly, their stability, as reported for uranyl compounds, e.g. autunite hydrated (Sowder et al. 2000).

Acknowledgements

The first specimen of nuragheite was kindly provided by Giuseppe Tanca; additional specimens were given by Fernando Caboni, Marzio Mamberti, and Antonello Vinci. Massimo Nespolo is thanked for electron microprobe analysis of nuragheite. The paper benefited of the comments by Stuart Mills, Sergey Krivovichev, and an anonymous reviewer.

References

Bindi, L., and Evain, M. (2007) Gram-Charlier development of the atomic displacement factors into mineral structures: The case of samsonite, $Ag_4MnSb_2S_6$. American Mineralogist, 92, 886–891.

Birch, W.D., Pring, A., McBriar, E.M., Gatehouse, B.M., and McCammon, C.A. (1998) Bamfordite, $Fe^{3+}Mo_2O_6(OH)_3 \cdot H_2O$, a new hydrated iron molybdenum oxyhydroxide from Queensland, Australia: description and crystal chemistry. American Mineralogist, 83, 172–177.

Bonaccorsi, E., and Orlandi, P. (2010) Tancaite-(Ce), a new molybdate from Italy. Acta Mineralogica Petrographica Abstract Series. 20th General Meeting of the International Mineralogical Association, 21st-27th August, 2010. Budapest, Hungary, 6, 494.

Boni, M., Stein, H.J., Zimmerman, A., and Villa, I.M. (2003) Re-Os age for molybdenite from SW Sardinia (Italy): A comparison with $^{40}Ar/^{39}Ar$ dating of Variscan granitoids. Mineral Exploration and Sustainable Development, Eliopoulos et al. (ed), 247–250.

Brese, N.E., and O'Keeffe, M. (1991) Bond-valence parameters for solids. Acta Crystallographica, B47, 192–197.

Buck, E.C., Wronkiewicz, D.J., Finn, P.A., and Bates, J.K. (1997) A new uranyl oxide hydrate phase derived from spent fuel alteration. Journal of Nuclear Materials, 249, 70–76.

Chiari, G., and Ferraris, G. (1982) The water molecule in cristalline hydrates studied by neutron diffraction. Acta Crystallographica, B38, 2331–2341.

Cremers, T.L., Eller, P.G., and Penneman, R.A. (1983) Orthorhombic Thorium(IV) Molybdate, $Th(MoO_4)_2$. Acta Crystallographica, C39, 1165–1167.

Dornberger-Schiff, K. (1964) Grundzüge einer Theorie der OD Strukturen aus Schichten. Abhandlungen der Deutschen Akademie der Wissenschaften zu Berlin, Kl. für Chemie, Geologie und Biologie, 3, 106 p.

Dornberger-Schiff, K. (1966) Lehrgang über OD Strukturen. Akademie Verlag, Berlin, 64 p.

Ferraris, G., and Ivaldi, G. (1988) Bond valence vs bond length in O···O hydrogen bonds. Acta Crystallographica, B44, 341–344.

Ferraris, G., Makovicky, E., and Merlino, S. (2004) Crystallography of Modular Materials. Oxford University Press.

Finney, J.J., and Rao, N.N. (1967) The crystal structure of cheralite. American Mineralogist, 52, 13–19.

Frondel, C. (1958) Systematic mineralogy of uranium and thorium. Geological Survey Bulletin, 1064, 400 p. U.S. Government Printing Office, Washington.

Grell, H., and Dornberger-Schiff, K. (1982) Symbols of OD groupoid families referring to OD structures (polytypes) consisting of more than one kind of layer. Acta Crystallographica, A38, 49–54.

Hazen, R.M., Ewing, R.C., and Sverjensky, D.A. (2009) Evolution of uranium and thorium minerals. American Mineralogist, 94, 1293–1311.

Holland, T.J.B., and Redfern, S.A.T. (1997) Unit cell refinement from powder diffraction data: the use of regression diagnostics. Mineralogical Magazine, 61, 65–77.

Kraus, W., and Nolze, G. (1996) PowderCell – a program for the representation and manipulation of crystal structures and calculation of the resulting X-ray powder patterns. Journal of Applied Crystallography, 29, 301–303.

Kuhs, W. F. (1992) Generalized atomic displacements in crystallographic structure analysis. Acta Crystallographica, A48, 80–98.

Larson, E.M., Eller, P.G., Cremers, T.L., Penneman, R.A., and Herrick, C.C. (1989) Structure of trigonal thorium molybdate. Acta Crystallographica, C45, 1669–1672.

Mandarino, J.A. (1979) The Gladstone-Dale relationship. Part III. Some general applications. Canadian Mineralogist, 17, 71-76.

Mandarino, J.A. (1981) The Gladstone-Dale relationship. Part IV. The compatibility concept and its application. Canadian Mineralogist, 19, 441–450.

Orlandi, P. (2013) Schulenbergite, minohlite, namuwite e osakaite nelle associazioni supergeniche del Distretto Minerario Schio-Recoaro (Vicenza). Micro, 11, 2–9.

Orlandi, P., Pasero, M., and Bigi, S. (2010) Sardignaite, a new mineral, the second known bismuth molybdate: description and crystal structure. Mineralogy and Petrology, 100, 17-22.

Orlandi, P., Demartin, F., Pasero, M., Leverett, P. Williams, P.A., and Hibbs, D.E. (2011) Gelosaite, $BiMo^{6+}_{(2-5x)}Mo^{5+}_{6x}O_7(OH)\cdot H_2O$ ($0 \leq x \leq 0.4$), a new mineral from Su Senargiu (CA), Sardinia, Italy, and a second occurrence from Kingsgate, New England, Australia. American Mineralogist, 96, 268–273.

Orlandi, P., Biagioni, C., Pasero, M., Demartin, F. and Campostrini, I. (2013a) Mambertiite, IMA 2013-098. CNMNC Newsletter No. 18, December 2013, page 3257. Mineralogical Magazine, 77, 3249–3258.

Orlandi, P., Gelosa, M., Bonacina, E., Caboni, F., Mamberti, M., Tanca, G.A. and Vinci, A. (2013b) Sardignaite, gelosaite et tancaite-(Ce): trois nouveaux minéraux de Su Seinargiu, Sarroch, Sardaigne, Italie. Le Règne Minéral, 112, 39–52.

Orlandi, P., Biagioni, C., Bindi, L., and Nestola, F. (2014) Ichnusaite, $Th(MoO_4)_2\cdot 3H_2O$, the first natural thorium molybdate: occurrence, description, and crystal structure. American Mineralogist, http://dx.doi.org/10.2138/am.2014.4844.

Oxford Diffraction (2006) CrysAlis RED (Version 1.171.31.2). Oxford Diffraction Ltd, Abingdon, Oxfordshire, England.

Petříček, V., Dušek, M., and Palatinus, L. (2006) JANA2006. The crystallographic computing system. Institute of Physics, Prague, Czech Republic.

Sheldrick, G.M. (2008) A short history of SHELX. Acta Crystallographica, A64, 112–122.

Sowder, A.G., Clark, S.B., and Fjeld, R.A. (2000) Dehydration of synthetic autunite hydrates. Radiochimica Acta, 88, 533–538.

Strunz, H., and Nickel, E.H. (2001) Strunz Mineralogical Tables. 9th Edition, E. Schweizerbart Verlag, Stuttgart, 870 p.

Suzuki, Y., Sato, T., Isobe, H., Kogure, T., and Murakami, T. (2005) Dehydration processes in the meta-autunite group minerals meta-autunite, metasaléeite, and metatorbernite. American Mineralogist, 90, 1308–1314.

Taylor, M., and Ewing, R.C. (1978) The crystal structure of the $ThSiO_4$ polymorphs: huttonite and thorite. Acta Crystallographica, B34, 1074–1079.

Trueblood, K.N., Bürgi, H.-B., Burzlaff, H., Dunitz, J.D., Gramaccioli, C. M., Schulz, H., Shmueli, U., and Abrahams, S.C. (1996) Atomic Dispacement Parameter Nomenclature. Report of a Subcommittee on Atomic Displacement Parameter Nomenclature. Acta Crystallographica, A52, 770-781.

Wilson, A.J.C. (1992) International Tables for X-ray Crystallography Volume C. Kluwer, Dordrecht.

Table captions

Table 1. Microprobe analyses (average of 6 spot analyses) of nuragheite (in wt%).

Table 2. Crystal data and summary of parameters describing data collection and refinement for nuragheite.

Table 3. Atomic positions and displacement parameters (in $Å^2$) for nuragheite.

Table 4. Selected bond distances (in Å) for nuragheite.

Table 5. X-ray powder diffraction data for nuragheite.

Table 6. Bond valence calculations according to bond-valence parameters taken from Brese and O'Keeffe (1991).

Table 7. Unit-cell parameters and space group symmetries for natural and synthetic thorium molybdates.

Figure captions

Fig. 1. Nuragheite, tabular {100} crystals with quartz.

Fig. 2. The crystal structure of nuragheite as seen down **c** (a) and **a** (b). Large polyhedra: grey = Th-centered polyhedra. Tetrahedra: light grey = Mo1 tetrahedra; dark grey = Mo2 tetrahedra. Light grey circles = H_2O groups.

Fig. 3. Hydrogen bonds in nuragheite. Large polyhedra: grey = Th-centered polyhedra. Tetrahedra: light grey = Mo1 tetrahedra; dark grey = Mo2 tetrahedra. Circles represent anion sites.

Fig. 4. Comparison between the crystal structures of ichnusaite (a) and nuragheite (b).

Fig. 5. Crystal structures of the two MDO polytypes of orthorhombic synthetic $Th(MoO_4)_2$ compound, as seen down **b**. The **c** axis is vertical, **a** horizontal.

443 **Table 1.** Microprobe analyses (average of 6 spot analyses) of nuragheite (in wt%).
444

Oxide	wt%	range	e.s.d.
MoO_3	49.38	47.24–51.43	1.46
ThO_2	45.39	43.93–46.90	1.19
H_2O_{calc}	3.09		
Total	97.86		

445
446

Table 2. Crystal data and summary of parameters describing data collection and refinement for nuragheite.

Crystal data	
X-ray formula	$Th(MoO_4)_2 \cdot H_2O$
Crystal size (mm^3)	0.20 x 0.10 x 0.05
Cell setting, space group	Monoclinic, $P2_1/c$
a (Å)	7.358(2)
b (Å)	10.544(3)
c (Å)	9.489(2)
β (°)	91.88(2)
V ($Å^3$)	735.8(3)
Z	4
Data collection and refinement	
Radiation, wavelength (Å)	Mo $K\alpha$, λ = 0.71073
Temperature (K)	293
$2\theta_{max}$	57.84
Measured reflections	3274
Unique reflections	1637
Reflections with $F_o > 4\sigma(F_o)$	1342
R_{int}	0.0684
$R\sigma$	0.1013
Range of h, k, l	$-9 \le h \le 9$, $-14 \le k \le 14$, $0 \le l \le 12$
R [$F_o > 4\sigma(F_o)$]	0.0775
R (all data)	0.0790
wR (on F_o^2)	0.1722
Goof	1.042
Number of least-squares parameters	105
Maximum and minimum residual peak (e $Å^{-3}$)	10.70 (at 0.75 Å from O8) -9.90 (at 0.95 Å from Mo2)

Note: the weighting scheme is defined as $w = 1/[\sigma^2(F_o^2) + (aP)^2 + bP]$, with $P = [2F_c^2 + \mathrm{Max}(F_o^2,0)]/3$. a and b values are 0.1080 and 0.

480
481 **Table 3**. Atomic positions and displacement parameters (in Å^2) for nuragheite.
482

Site	*x*	*y*	*z*	U_{eq}	U_{11}	U_{22}	U_{33}	U_{23}	U_{13}	U_{12}
Th	0.7298(1)	0.5456(1)	0.2447(1)	0.0156(3)	0.0164(4)	0.0163(4)	0.0142(4)	-0.0006(3)	0.0009(4)	-0.0004(3)
Mo1	0.6241(3)	0.2408(2)	0.0018(2)	0.0174(4)	0.0187(10)	0.0177(8)	0.0159(9)	0.0002(7)	0.0012(10)	-0.0002(10)
Mo2	0.7864(3)	0.5922(5)	-0.1842(2)	0.0174(5)	0.0186(12)	0.0182(8)	0.0154(10)	-0.0011(7)	0.0014(9)	-0.0023(9)
O1	0.560(3)	0.556(2)	-0.239(2)	0.025(4)	0.033(11)	0.028(8)	0.015(9)	-0.001(7)	-0.007(10)	0.004(8)
O2	0.948(2)	0.481(1)	-0.239(2)	0.011(3)	0.012(7)	0.010(6)	0.010(7)	0.001(6)	-0.002(7)	-0.001(5)
O3	0.844(2)	0.742(2)	-0.262(2)	0.020(3)	0.018(8)	0.021(7)	0.020(8)	0.002(7)	-0.005(8)	-0.007(7)
O4	0.759(3)	0.125(1)	-0.077(2)	0.017(3)	0.017(10)	0.016(6)	0.017(7)	-0.010(6)	-0.006(7)	0.009(7)
O5	0.494(3)	0.329(2)	-0.125(2)	0.021(4)	0.021(11)	0.018(7)	0.023(9)	-0.002(7)	0.010(7)	0.006(8)
O6	0.461(3)	0.160(2)	0.088(2)	0.024(4)	0.029(11)	0.019(8)	0.026(9)	0.000(7)	0.003(8)	-0.005(8)
Ow7	0.895(3)	0.619(2)	0.478(2)	0.020(4)	0.014(10)	0.030(8)	0.015(8)	0.005(7)	0.002(7)	-0.002(8)
O8	0.792(4)	0.599(2)	0.005(2)	0.036(5)						
O9	0.760(3)	0.343(1)	0.113(1)	0.076(4)	0.027(11)	0.008(6)	0.012(7)	-0.006(5)	-0.006(7)	-0.003(7)

Table 4. Selected bond distances (in Å) for nuragheite.

Th	–O5	2.37(2)	Mo1	–O6	1.71(2)
	–O1	2.39(2)		–O4	1.75(2)
	–O2	2.39(2)		–O5	1.77(2)
	–O3	2.40(2)		–O9	1.79(1)
	–O8	2.40(2)		average	1.76
	–O6	2.46(2)	Mo2	–O2	1.76(2)
	–O4	2.48(1)		–O1	1.77(2)
	–O9	2.49(1)		–O8	1.78(2)
	–Ow7	2.60(2)		–O3	1.80(2)
	average	2.44		average	1.78

Table 5. X-ray powder diffraction data for nuragheite.

I_{obs}	d_{obs}	I_{calc}	d_{calc}	*h k l*	I_{obs}	d_{obs}	I_{calc}	d_{calc}	*h k l*
w	7.4*	18	7.35	1 0 0	w	2.775*	13	2.770	1 1 3
w	7.1*	5	7.05	0 1 1	vw	2.738*	3	2.711	0 2 3
w	6.1*	11	6.03	1 1 0	w	2.673*	10	2.653	-1 3 2
m	**5.28***	19	5.27	0 2 0	vw	2.620*	6	2.618	1 3 2
m	**5.20***	42	5.15	-1 1 1	w	2.597*	14	2.576	-2 2 2
m	**5.04***	47	5.03	1 1 1	w	2.553*	6	2.540	0 4 1
m	**4.756***	34	4.742	0 0 2			9	2.514	2 2 2
w	4.304*	8	4.285	1 2 0	vw	2.394	5	2.388	3 1 0
w	3.890	8	3.927	1 0 2			18	2.371	0 0 4
		11	3.877	1 2 1			7	2.333	-3 1 1
mw	3.824*	40	3.778	-1 1 2	w	2.300	6	2.302	2 1 3
m	**3.688**	29	3.680	1 1 2			11	2.298	3 1 1
		46	3.677	2 0 0	w	2.277*	7	2.255	-1 3 3
vs	**3.546***	100	3.526	0 2 2	w	2.228*	9	2.223	1 3 3
mw	3.479*	14	3.472	2 1 0	vw	2.154*	9	2.153	2 2 3
mw	3.231	14	3.228	2 1 1	w	2.088*	8	2.081	2 4 1
		12	3.210	-1 2 2			5	2.036	-3 2 2
s	**3.177***	79	3.171	1 3 0	w	2.034	8	2.027	1 5 0
		10	3.028	0 1 3			7	2.024	0 4 3
		12	3.020	-1 3 1			7	2.023	-2 0 4
m	**3.024**	25	3.016	2 2 0	vw	1.930			
		9	2.995	1 3 1	mw	1.883			
		22	2.953	-2 0 2	w	1.770			
		12	2.861	2 0 2	w	1.743			
mw	2.859	10	2.844	-2 1 2					
		9	2.832	-1 1 3					

Notes: the d_{hkl} values were calculated on the basis of the unit cell refined by using single-crystal data. Intensities were calculated on the basis of the structural model using the software PowderCell (Kraus and Nolze, 1996). Observed intensities were visually estimated. vs = very strong; s = strong; m = medium; mw = medium-weak; w = weak; vw = very weak. Only reflections with I_{calc} > 5 are listed, if not observed.The strongest reflections are given in bold. Reflections used for the refinement of the unit-cell parameters are indicated by an asterisk.

497

498 **Table 6**. Bond valence calculations according to bond-valence parameters taken from Brese
499 and O'Keeffe (1991).
500

Site	O1	O2	O3	O4	O5	O6	Ow7	O8	O9	Σ (X–O)
Th	0.55	0.55	0.53	0.43	0.58	0.45	0.31	0.53	0.42	4.35
Mo1				1.53	1.45	1.70			1.37	6.05
Mo2	1.37	1.45	1.34					1.49		5.65
Σ (O–X)	1.92	2.00	1.87	1.96	2.03	2.15	0.31	2.02	1.79	
Σ (O–X)*	1.92	2.00	2.05	2.20	2.03	2.15	-0.11	2.02	1.79	
Species	O	O	O	O	O	O	H_2O	O	O	

*after correction for O···O hydrogen bonds.

501
502
503 **Table 7**. Unit-cell parameters and space group symmetries for natural and synthetic thorium
504 molybdates.

Name	Chemical formula	*a* (Å)	*b* (Å)	*c* (Å)	α (°)	β (°)	γ (°)	*V* (Å^3)	s.g.	Ref.
Ichnusaite	$Th(MoO_4)_2{\cdot}3H_2O$	9.680	10.377	9.378	90	90	90	942.0	$P2_1/c$	[1]
Nuragheite	$Th(MoO_4)_2{\cdot}H_2O$	7.358	10.544	9.489	90	91.88	90	735.8	$P2_1/c$	[2]
Synthetic	$Th(MoO_4)_2$	10.318	9.737	14.475	90	90	90	1454.0	*Pbca*	[3]
Synthetic	$Th(MoO_4)_2$	17.593	17.593	6.238	90	90	120	1672.2	*P*-3	[4]

505 [1] Orlandi et al. (2014); [2] this work; [3] Cremers et al. (1983); [4] Larson et al. (1989).
506

507 **Fig. 1**. Nuragheite, tabular {100} crystals with quartz.
508

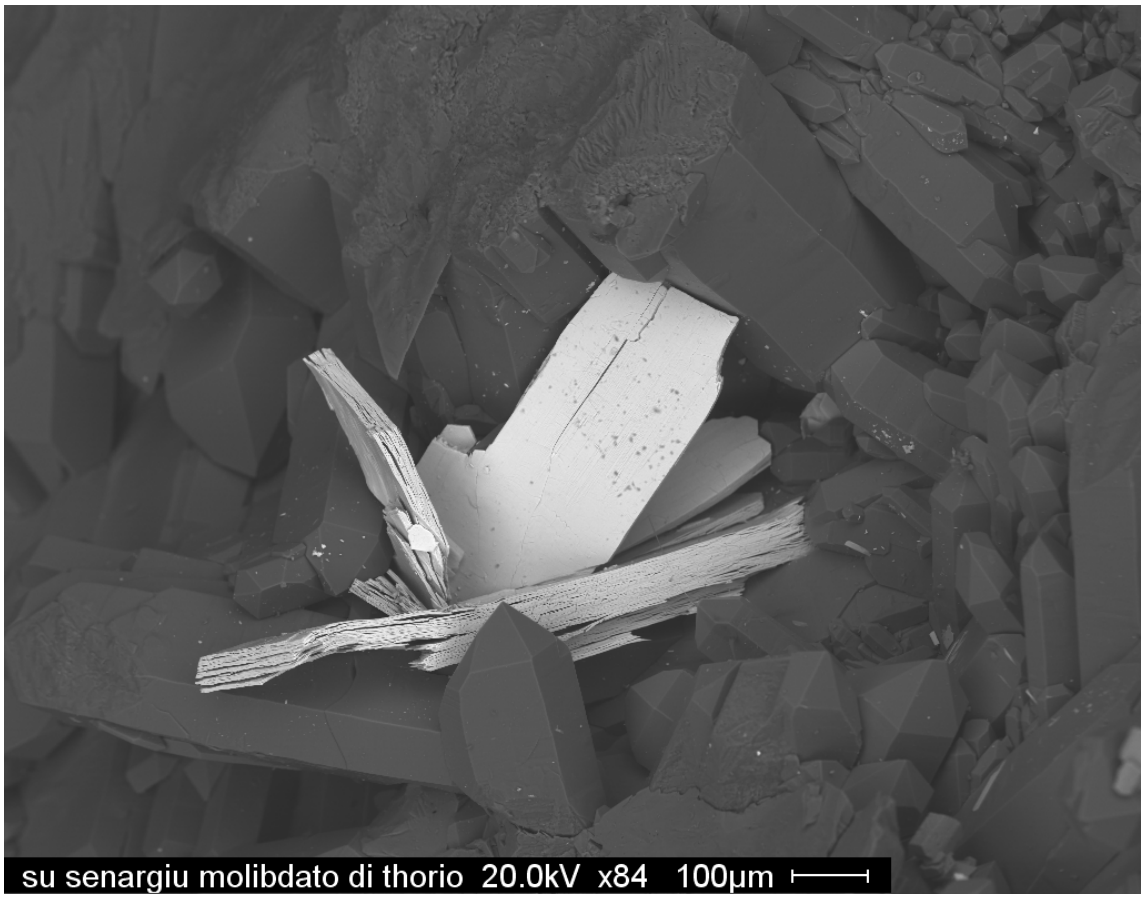

509
510
511

512 **Fig. 2**. The crystal structure of nuragheite as seen down **c** (a) and **a** (b). Large polyhedra: grey
513 = Th-centered polyhedra. Tetrahedra: light grey = Mo1 tetrahedra; dark grey = Mo2
514 tetrahedra. Light grey circles = H_2O groups.
515

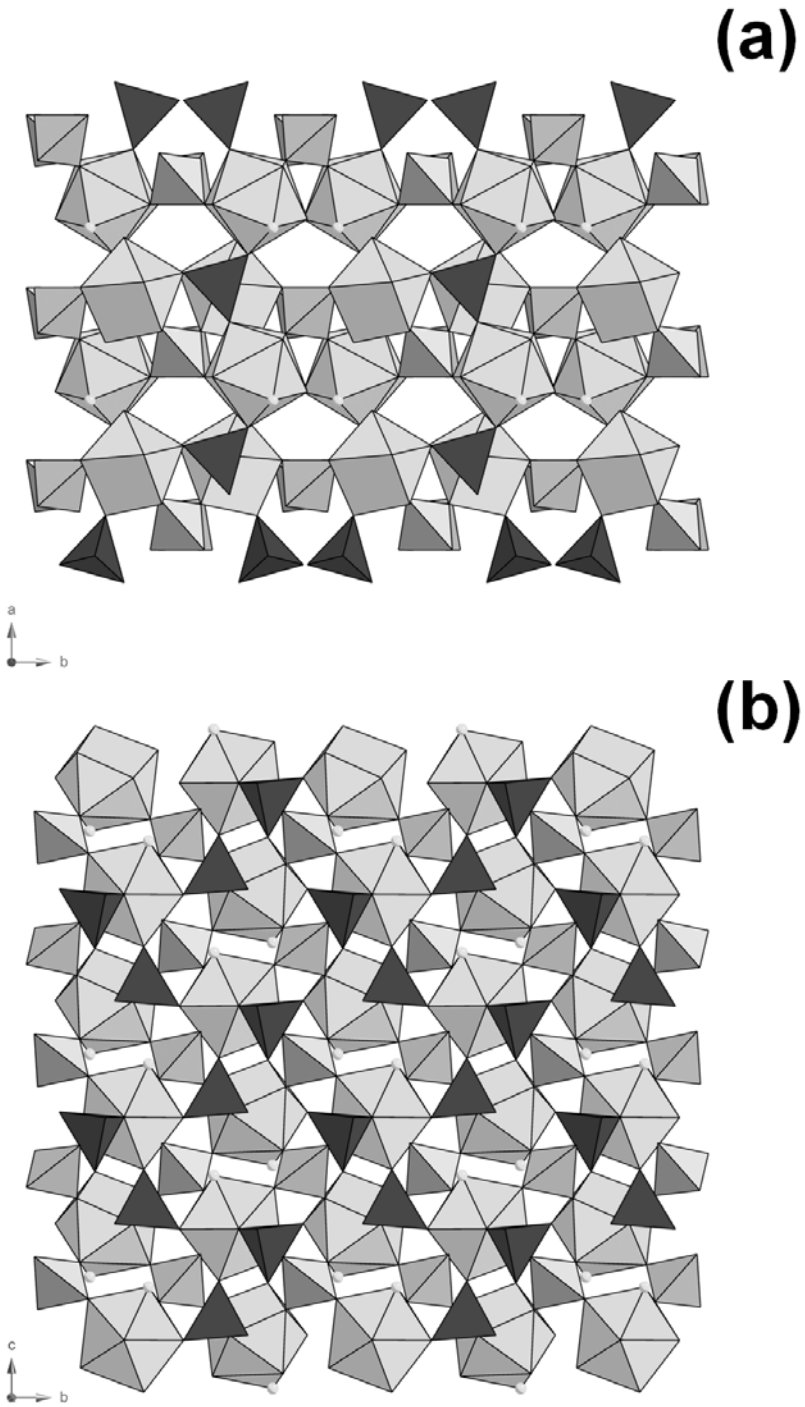

516

517
518 **Fig. 3**. Hydrogen bonds in nuragheite. Large polyhedra: grey = Th-centered polyhedra.
519 Tetrahedra: light grey = Mo1 tetrahedra; dark grey = Mo2 tetrahedra. Circles represent anion
520 sites.

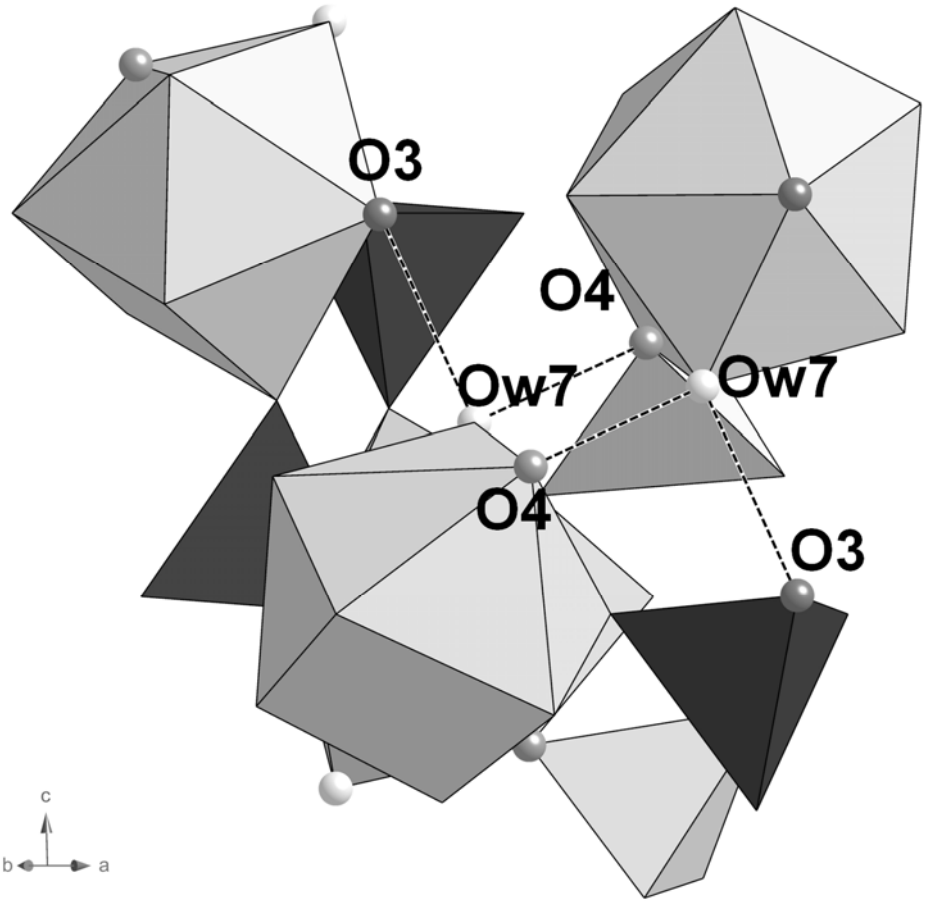

521
522

523 **Fig. 4**. Comparison between the crystal structures of ichnusaite (a) and nuragheite (b).

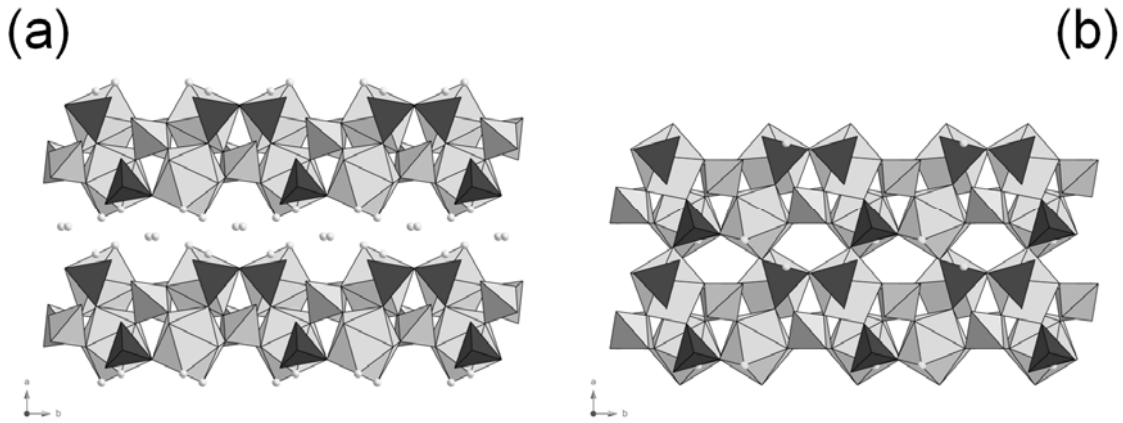

524
525

526 **Fig. 5**. Crystal structures of the two MDO polytypes of orthorhombic synthetic $Th(MoO_4)_2$
527 compound, as seen down **b**. The **c** axis is vertical, **a** horizontal.

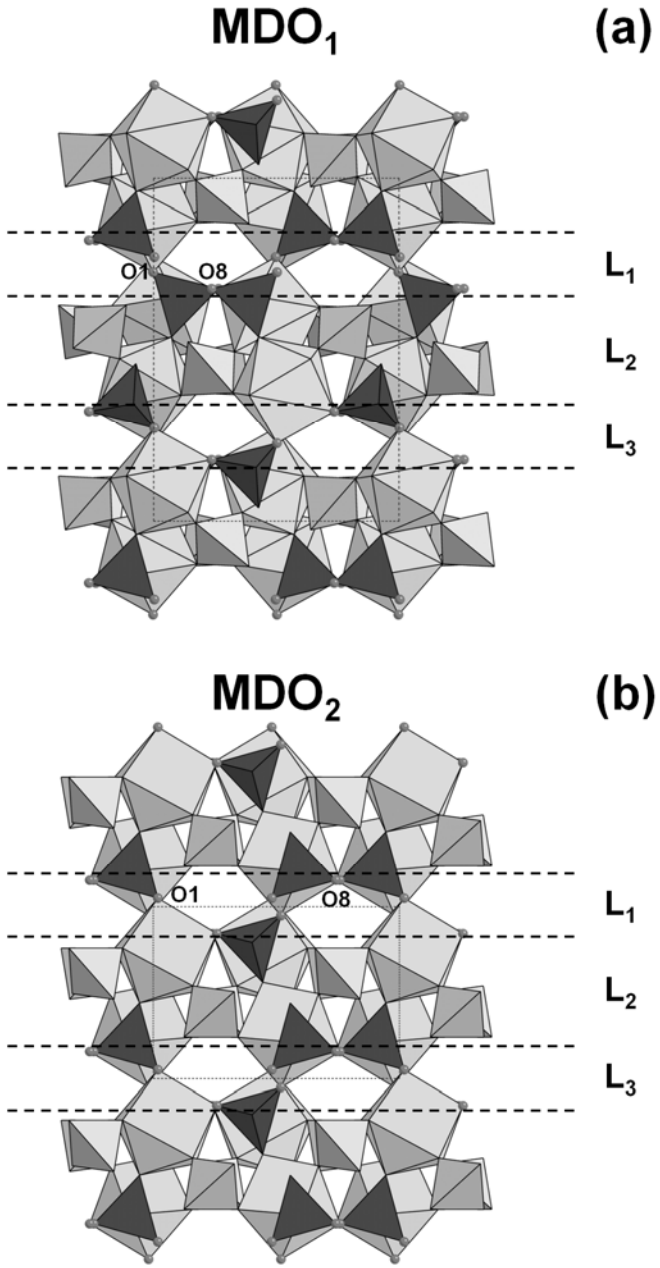

528
529

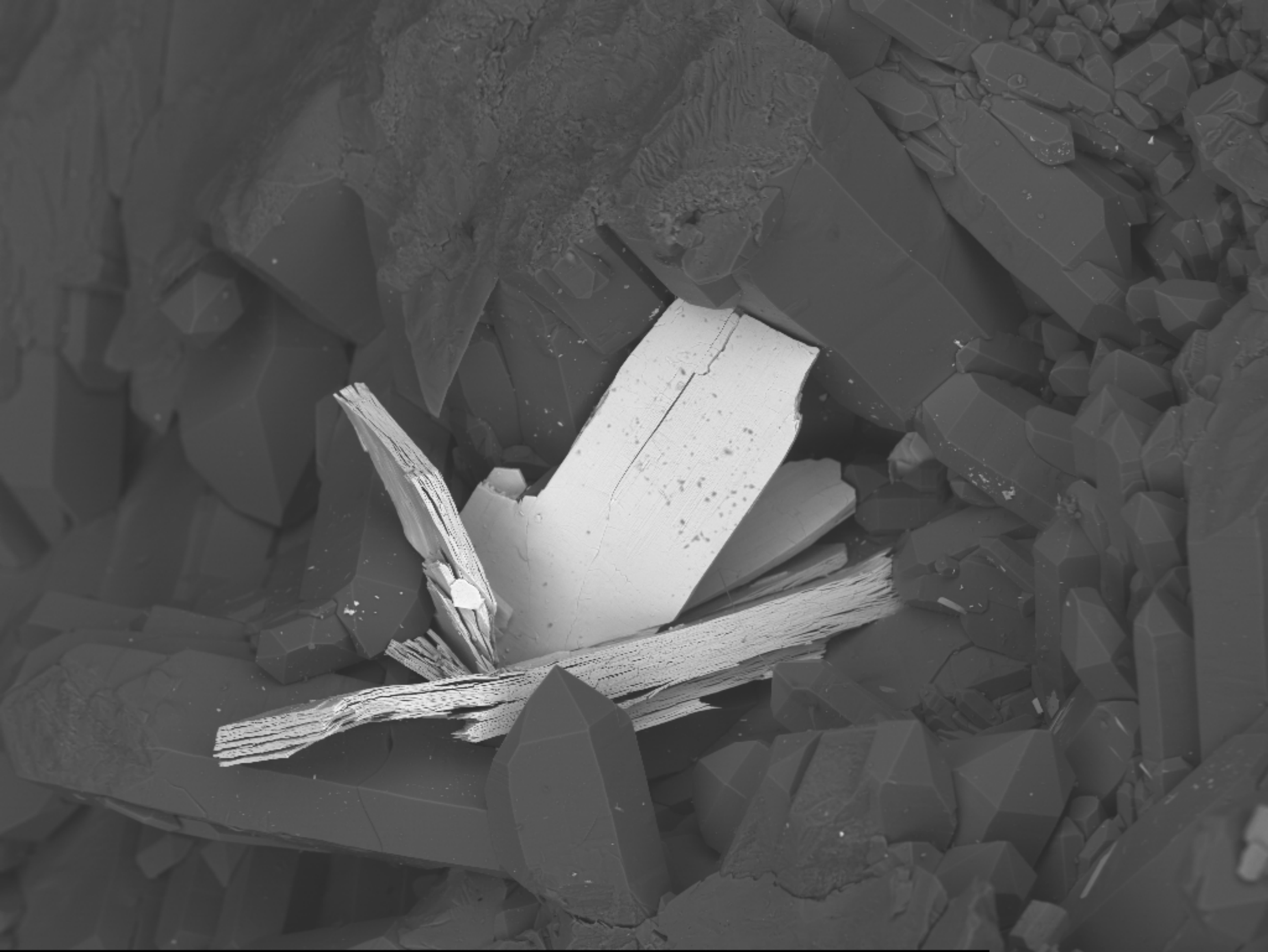
su senargiu molibdato di thorio 20.0kV x84 100µm

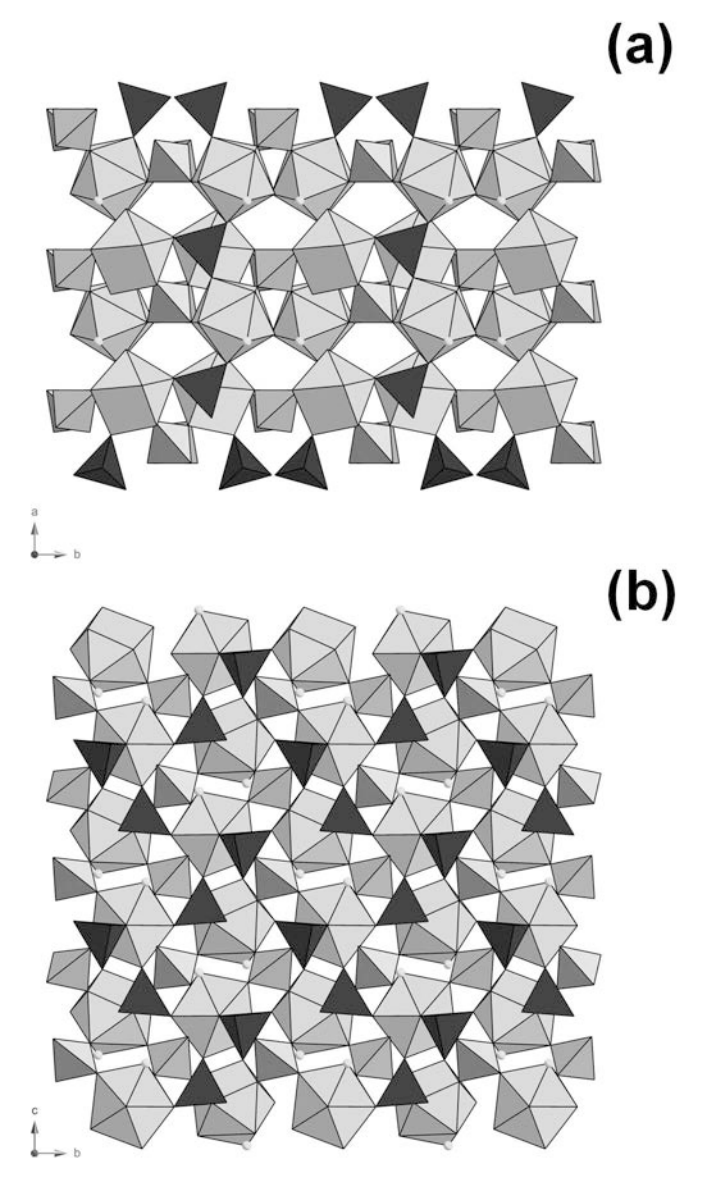
(a)
a
b
(b)
c
b

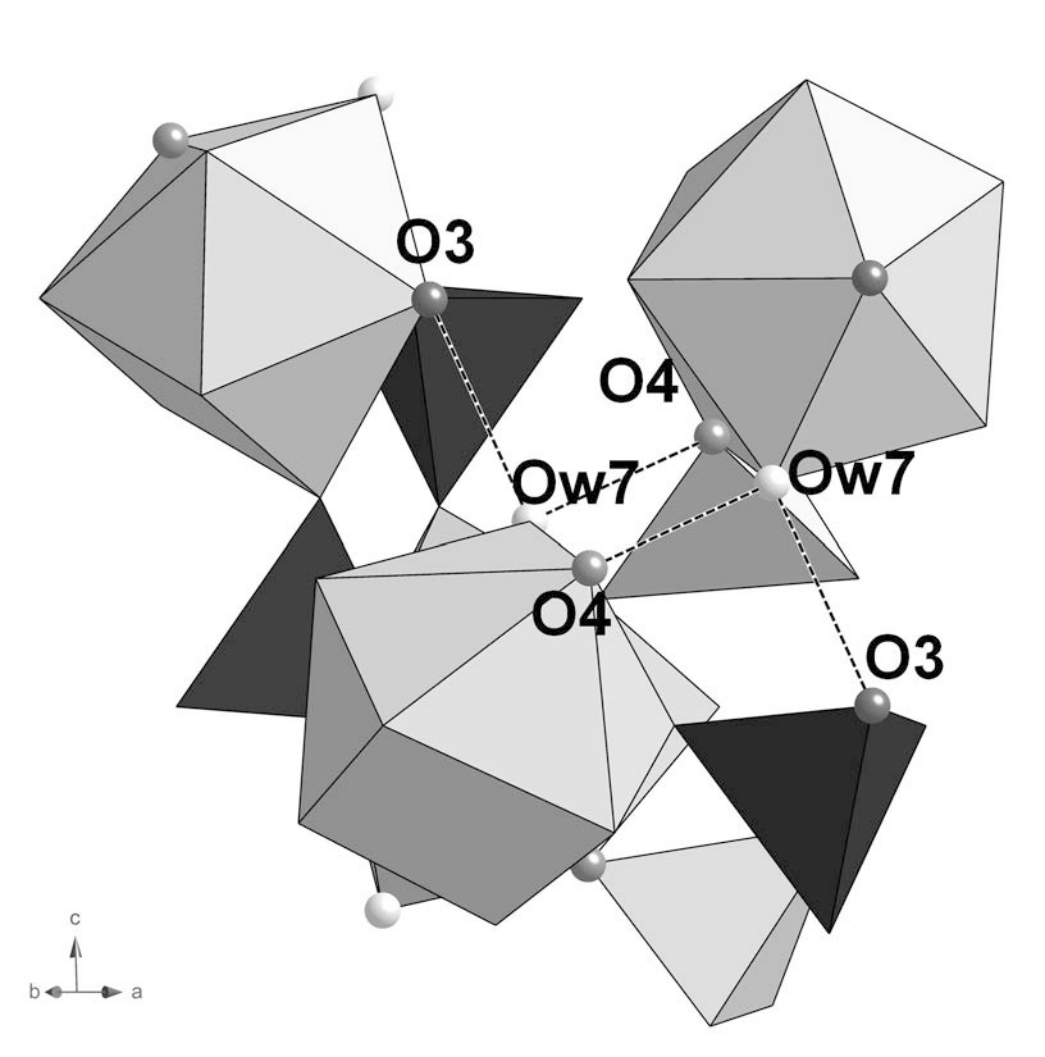
O3
O4
Ow7
Ow7
O4
O3
c
b
a

(a)

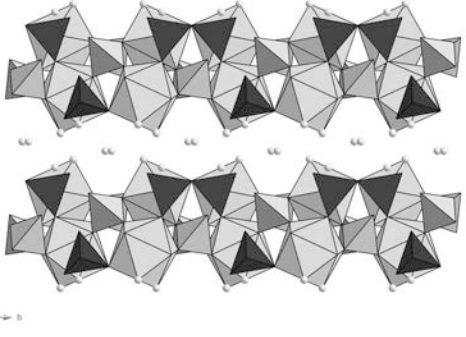

(b)

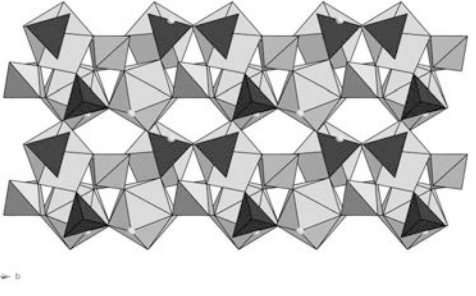

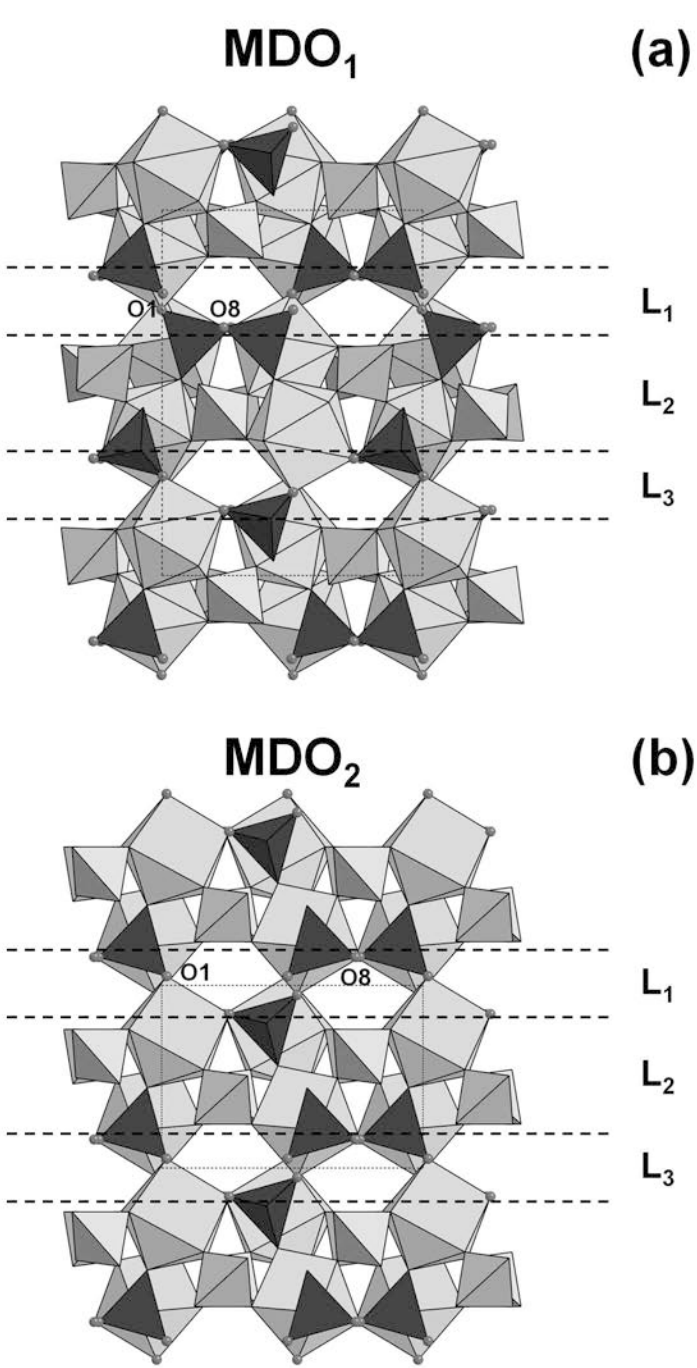
MDO1
(a)
O1
O8
L1
L2
L3
MDO2
(b)
O1
O8
L1
L2
L3